Geomechanics and Engineering, *Vol. 26, No. 5 (2021) 441-452*
https://doi.org/10.12989/gae.2021.26.5.441

Recognition and prevention of rockfall vulnerable area in open-pit mines based on slope stability analysis

Chun Zhu[1,2], Manchao He[2], Zhigang Tao[2], Qingxiang Meng*[3] and Xiaohu Zhang[4]

[1]*School of Earth Sciences and Engineering, Hohai University, Nanjing, 210098, China*
[2]*State Key Laboratory for Geomechanics & Deep Underground Engineering, Beijing 100083, China*
[3]*Research Institute of Geotechnical Engineering, Hohai University, Nanjing 210098, Jiangsu, China*
[4]*School of Civil Engineering, Guizhou University of Engineering Science, Bijie, Guizhou, 551700, China*

(Received April 12, 2021, Revised July 8, 2021, Accepted August 11, 2021)

Abstract. Because of a wide distribution range, sudden occurrence, and high frequency of rockfall disasters on the slope of open-pit mines, it is difficult to effectively control the rockfall disasters in open-pit mines. The slope stabilities of slopes of 13 typical sections in the Changshanhao open-pit mine were calculated using 3DEC software, and the vulnerable area of each slope section was determined. These areas were analyzed as high-incidence areas of rockfalls. Combined with the field geological conditions, the slopes of the W6 and W8 sections where rockfall disasters easily occur were selected to study the motion characteristics of rockfalls, including the trajectory, landing distribution, bouncing height, and total kinetic energy using Rocfall software. According to different distribution characteristics of high-incidence areas of rockfall disasters on a slope, the gravel cushion and protective net methods are proposed to control rockfall disasters. The effectiveness and reasonableness of prevention methods were validated using numerical simulation, proving a good basis for scientific prevention and control of rockfall disasters in open-pit mines.

Keywords: gravel cushion; rockfalls; slope vulnerable area; stability analysis; 3DEC software

1. Introduction

The phenomenon of rockfalls refers to the dynamic evolution of individual rocks rapidly moving downwards when they become unstable on a sloped surface, finally impacting obstacles or stopping in flat zones. When the surface of an open-pit slope is severely weathered and there are strong mining disturbances and rainfall, rockfalls are observed in areas where dangerous rock mass is developed, severely threatening the safety of mining activity and workers.

Through laboratory tests, theoretical analysis, and numerical simulation, the motion characteristics of rockfalls have been widely evaluated (Zhu *et al.* 2019, Gischig *et al.* 2015, Andrew and Oldrich 2017, Bourrier *et al.* 2009, Buzzi *et al.* 2012, James 2015, Spadari *et al.* 2012, Li *et al.* 2016, Hu *et al.* 2018, Gao *et al.* 2018a, b). According to friction theory, Zhang *et al.* (2015) calculated the tangential force and tangential coefficient of restitution (COR). Zhu *et al.* (2018 and 2021a) conducted many collision experiments between rockfalls and cushions to study the influences that the thickness and particle size of the cushion have on the energy consumption of rockfalls. To determine the hazardous rockfall zones and to select the control measures to improve the safety of steep mountain roads in the Kingdom of Saudi Arabia, rockfall hazard rating research was carried out (Maerz *et al.* 2015). Rosa *et al.* (2016) proposed a procedure to evaluate the risk caused by rockfalls; 103 cases of rockfall events were used to calibrate and validate rockfall modeling. Lam *et al.* (2018) developed a new displacement-based method to evaluate the overturning stability of rigid L-shaped barriers under the impact of rockfalls. Fano *et al.* (2019) proposed comprehensive evaluation criteria for rockfall disasters; this provides a complete understanding of rockfall disasters that can help authorities adopt proper methods to prevent rockfalls. Tan *et al.* (2018) conducted impact tests using blocks that had different diameters and a flexible barrier; the interaction between falling blocks and the flexible barrier was researched. To study the possibility of rocks falling onto railway tracks, Megan *et al.* (2018) proposed an approach for simulating rockfall hazards; the simulation results can be related to the rockfall events to provide a more realistic estimate of the hazard. Zhu *et al.* (2021b) built a numerical model of a rockfall impacting a cushion, and the impact force and penetration depth during collision between the rockfall and cushion were studied. Akin *et al.* (2021) built a 3-D rockfall model to evaluate the efficiency of rockfall ditches against rockfall disasters, and it was found that the effectiveness of a catchment ditch is highly dependent upon its depth. Yu *et al.* (2021) carried out a numerical simulation and tested a typical flexible barrier system; the dynamic responses of flexible rockfall barriers under the collision of blocks with different shapes were analyzed.

At present, although many protection methods have been developed and their effectiveness and reasonableness

*Corresponding author, Associate Professor
E-mail: mqx@hhu.edu.cn

ISSN: 2005-307X (Print), 2092-6219 (Online)

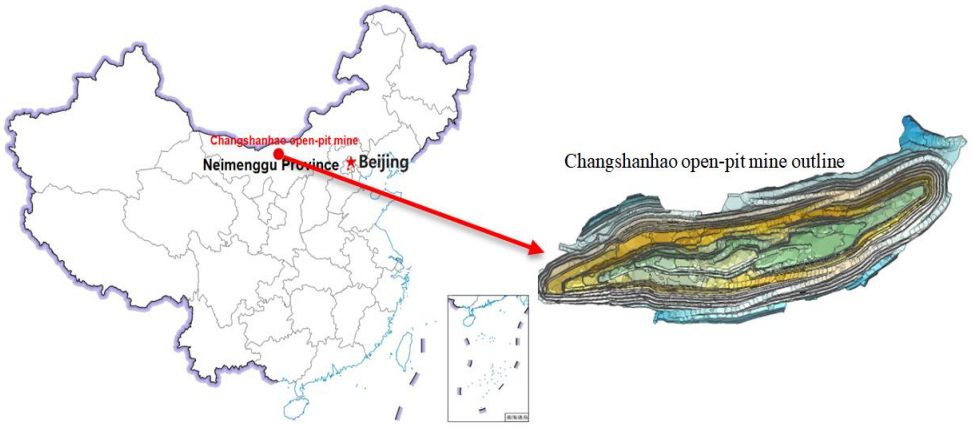

Fig. 1 Geographical location map of Changshanhao open-pit mine

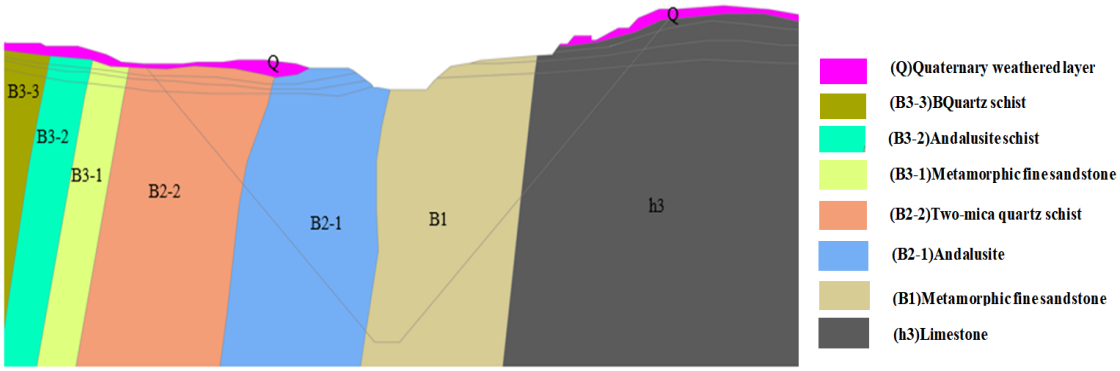

Fig. 2 Stratum distribution in Changshanhao open-pit mine (Tao *et al.* 2020)

have been validated (Bertolo *et al.* 2009, Bhatti 2018, Xu *et al.* 2018, Lambert *et al.* 2018; Laura *et al.* 2018, Anna *et al.* 2017, Koo *et al.* 2017), protection costs are relatively high because of a wide distribution range, sudden occurrence, and high frequency of rockfall disasters on the slopes of open-pit mines. It is difficult to effectively control rockfall hazards in open-pit mines. According to the engineering geological conditions of a mining area, the slope stability of an open-pit mine was analyzed using 3DEC software. Vulnerable slope areas were determined to obtain the initial moving point of rockfall disasters. Reasonable corresponding methods were used to control the rockfall disasters according to different distribution characteristics of rockfalls on the slopes of vulnerable areas.

2. Engineering background

2.1 Geographical location

The Changshanhao open-pit mine is located in Neimenggu province, China. The mine has a gently rolling denuded topography of low mountains and hills. The elevation ranges from 1,550 m to 1,750 m, and the relative elevation difference is 50–200 m, as shown in Fig. 1. Generally, the elevation is high in the east and low in the west, and its ore bodies are mainly distributed in the low-lying areas. Within this area, the rock strata are well exposed without vegetation cover.

2.2 Regional geological characteristics

As seen in Fig. 2, the main lithological compositions in the area include gneiss, andalusite schist, meta-sandstone, two-mica quartz schist, quartzite, and limestone. The north slope of the southwest stope of the ore field is dominated by slate and schist, and the south slope is dominated by limestone. The inclination of bedding planes is about 65°-85°. The north side of the mine is dominated by slate and schist, and the south side is dominated by limestone (Tao *et al.* 2019; Zhu *et al.* 2020). This area is subject to tectonic control, the slopes have a poor rock mass integrity, and the stability of rocks and ores is relatively weak. Therefore, there are many local landslides, collapses, and rockfall disasters during mining; it is essential to identify and control areas that are vulnerable to rockfalls.

2.3 Hydrogeological characteristics

The mine falls within a hilly plateau of a hydrogeological area that is characterized by a dry climate with slight precipitation and intense evaporation. The rainy season is mainly from July to September. The annual rainfall is 233.7 mm, and the annual evaporation is 2,646.2 mm. The lithology of the ore field and the surrounding strata are dominated by clastic rocks with a slightly soluble material. A weathering fissure aquifer based on clastic rocks exists only in a thin superficial stratum; the groundwater type is vein water within a faulted structure crushed zone.

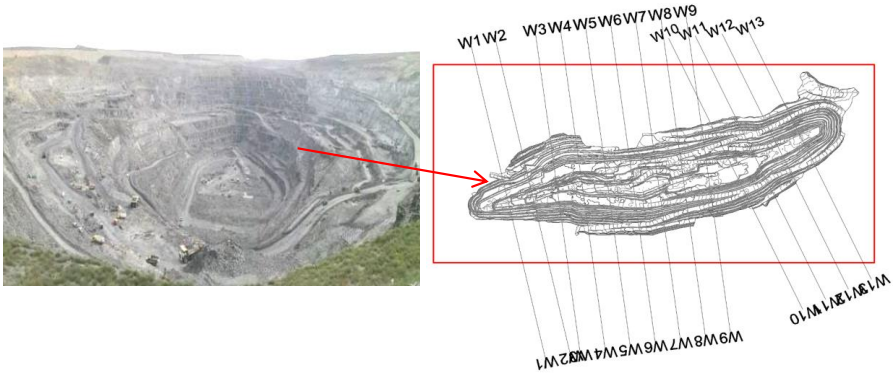

Fig. 3 Interception position plane of calculation section in southwest stope

(a) Direct shear test (b) Uniaxial compressive strength test

Fig. 4 Test process of mechanics strength parameters or rocks (Tao *et al.* 2020)

Therefore, as a whole, the ore field is basically not influenced by rainfall and groundwater (Zhu *et al.* 2020, 2021c).

3. Stability analysis of a slope in the Changshanhao open-pit mine

3.1 Selection of calculation section slopes

According to the distribution of rock strata, the north and south sides of the southeast stope can be divided into 13 sections for calculation. These sections are along the main axis of the stope with an average interval of 150 m. The north and south sides of 13 cross-sections were selected as the research object to study the slope stability. The north and south sides of the slope were studied to easily evaluate the main instability area of the slope, preventing the negligence or omission of some sliding areas in the design process. The specific section selection is shown in Fig. 3.

3.2 Analysis of numerical simulation

A direct shear apparatus and uniaxial compressive strength testing machine were used to study the mechanical properties of rock samples that were retrieved from the mining area, and the mechanics strength parameters of the rocks were determined (Figure 4).

3DEC software was used to analyze the slope stability of 13 cross-sections, and the initial crack growth may be ignored in this case. The parameters of the slope model were set (Table 1) according to the mechanical properties of the field slope rocks, and all of the experiments followed the rock mechanical test code recommended by the International Society of Rock Mechanics and Rock Engineering (ISRM). The displacement calculation results of 13 cross-sections are shown in Fig. 5.

(1) According to the stability analysis of the slopes of the W1–W14 sections, the areas are located at a U-shaped mouth on the west side of the southwest stope. The slope stability is relatively stable under the current mining pattern, and there is no large-scale sliding failure.

(2) By calculating the stability of the slopes of the W5–W7 sections, it is found that the areas are located at the 450 m range on the west side of the stope middle line. There is no large-scale sliding under the current mining conditions, and only the upper parts of the W6 and W7 sections show shallow sliding with a damage depth of 7 m.

(3) Through the calculations of the slope of the W8 section, it is found that the area is located in the middle of the southwest stope. The lower slope foot on the north side is a combined fractured zone, and an extrusion fracture zone with a damage depth of 10 m appears in the slope.

(4) From the analysis of the slopes of the W9–W11 sections, it is found that the areas are located at the 450 m range of the east side of the stope middle line. There is no large-scale sliding failure under the current mining conditions.

Table 1 Rock strength parameters in the 3DEC calculation model of the Changshanhao mine

Material code	lithology	Density/kg·m^{-3}	Bulk modulus (GPa)	shear modulus (GPa)	Cohesive force (MPa)	Friction angle (°)
Q	Quaternary	2000	51.53	21.08	1.50	45.00
FH	Weathering layer	2560	42.61	26.81	2.30	48.00
r	Granite	2600	140.11	72.24	11.00	56.00
B4	Andalusite schist-1	2840	117.13	65.95	12.00	49.00
B3-3	Black quartzite	2282	97.99	70.75	12.50	51.00
B3-2	Andalusite schist-2	2840	139.96	70.25	11.90	52.00
B3-1	Fine-grained sandstone-1	2750	137.13	69.95	13.50	51.30
B2-2	Dimica quartz schist	2845	81.05	68.32	14.20	54.00
B2-1	Andalusite schist-3	2842	80.53	63.69	18.20	55.00
B1	Fine-grained sandstone-2	2748	121.62	71.93	15.60	56.00
h3	Limestone	2830	137.13	69.95	16.40	54.00

(5) By calculating the stability of the slopes of the W12 and W13 sections, it is found that the areas are located at the U-shaped mouth on the east side of the southwest stope. Under the current conditions, there is no large-scale sliding

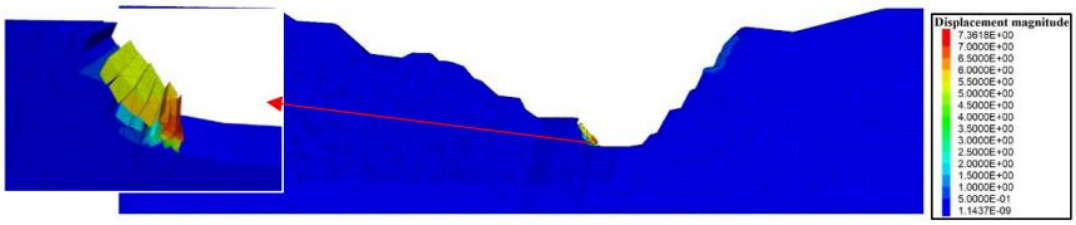

(a) Displacement contour of W1 section slope

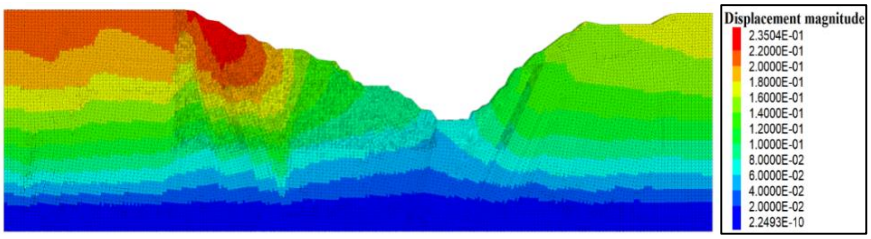

(b) Displacement contour of W2 section slope

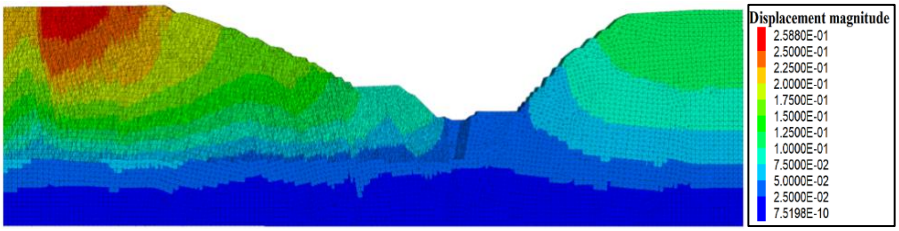

(c) Displacement contour of W3 section slope

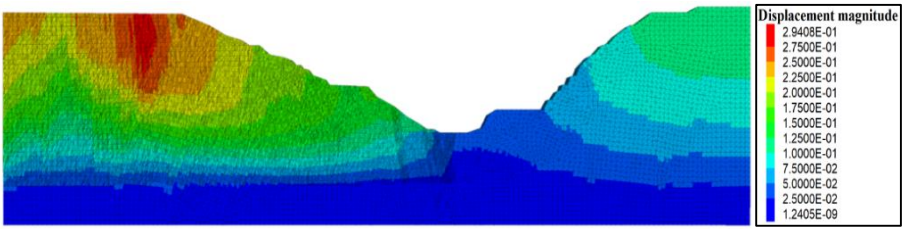

(d) Displacement contour of W4 section slope

Fig. 5 Displacement contour of each section slope

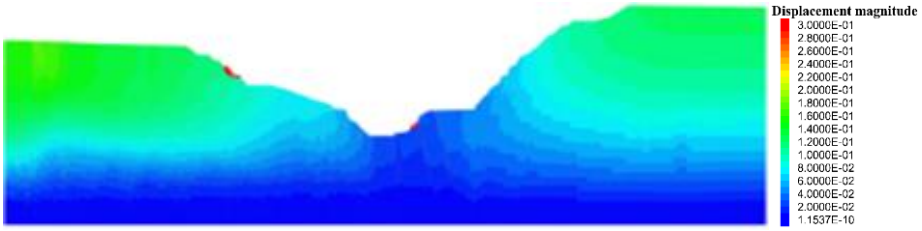

(e) Displacement contour of W5 section slope

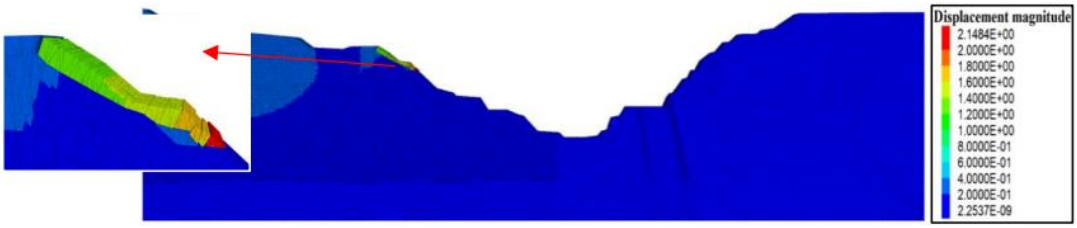

(f) Displacement contour of W6 section slope

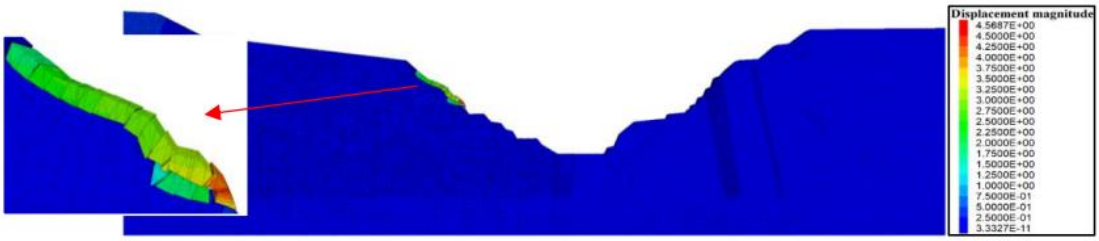

(g) Displacement contour of W7 section slope

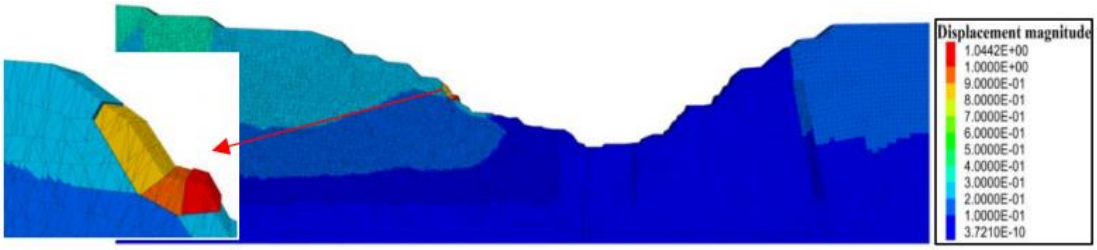

(h) Displacement contour of W8 section slope

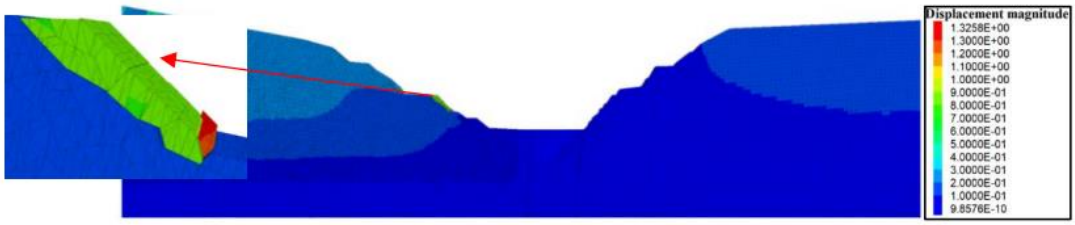

(i) Displacement contour of W9 section slope

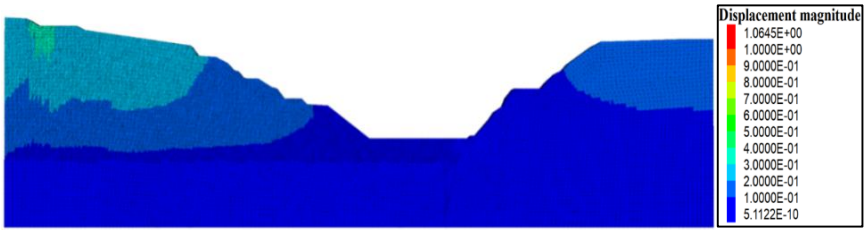

(j) Displacement contour of W10 section slope

Fig. 6 Continued

failure in the two sections. However, a sliding zone was observed along the north side of the W13 section slope. Also, the degree of failure gradually decreased from the fracture surface to the deep part, and this indicates that a large-scale sliding failure may occur.

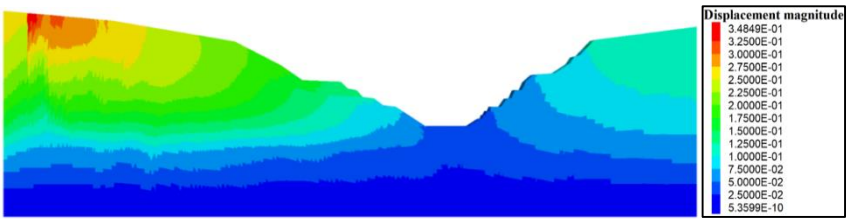

(k) Displacement contour of W11 section slope

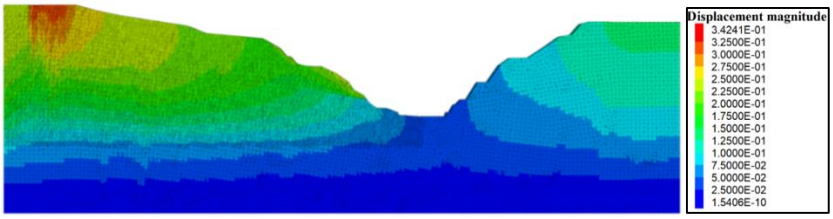

(l) Displacement contour of W12 section slope

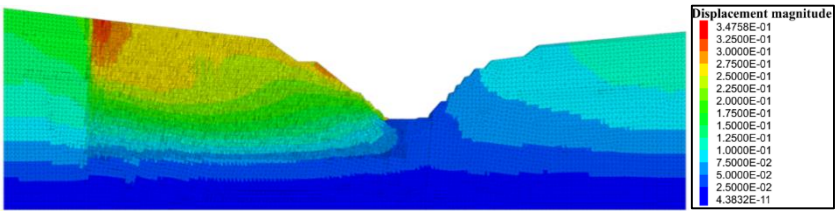

(m) Displacement contour of W13 section slope

Fig. 6 Continued

From the above analysis, it was observed that the slopes of the W1, W6, W7, W8, W9, and W13 sections have vulnerable slope areas that have a great possibility of rock collapse and occurrence of rockfalls. Overall, the slopes of the W6 and W8 sections are relatively prone to rockfalls disasters. Therefore, the slopes of these two sections were selected for evaluating the motion characteristics of rockfalls using Rocfall software. Reasonable corresponding control measures were used to prevent and control rockfalls, and the effectiveness of the control measures was determined using Rocfall.

4. Motion characteristics and prevention methods for rockfalls

Under the influence of weathering, rainfall, and mining activities, rockfall disasters in the Changshanhao mining area are frequent, as shown in Fig. 6. Thus, it is essential to use effective methods to control rockfall disasters.

4.1 Definition of coefficients of restitution

When a rockfall collides with the slope (Fig. 7), the COR can be defined as Eq. (1) according to the theory of inelastic collision (Zhu *et al.* 2019):

$$V_{COR} = \frac{V_2}{V_1} \tag{1}$$

where V_1 (m/s) is the incident velocity value before the collision and V_2 (m/s) is the rebound velocity value after the collision.

The kinematic COR can be divided into normal and tangential parts. In practice, the normal (R_n) and tangential (R_t) coefficients of restitution are widely defined as follows:

$$R_n = \frac{V_{n2}}{V_{n1}} \qquad R_t = \frac{V_{t2}}{V_{t1}} \tag{2}$$

where V_{n1} and V_{n2} are the normal parts, and V_{t1} and V_{t2} are the tangential parts of a rockfall's velocity before and after the collision, respectively (all in *m/s*).

4.2 Simulation and analysis of motion characteristics of rockfalls

Rocfall is a computer program based on the motion and collision theory (Yilmaz *et al.* 2008). Rocfall software specifies the material attributes of a slope and determines the starting position, quantity, and quality of rockfalls. The path of rockfalls can be then calculated. The kinetic energy, velocity, and jumping height of rockfalls at each point of a selected section can also be calculated. Rocfall can also be used to assist in determining protective measures. The material of each section of slope can be changed, and analysis to compare the results can be conducted using Rocfall. Therefore, Rocfall was used in this research to explore the movement characteristics of rockfalls and to assess the rationality of protective measures.

Andalusite schist is the main rock mass in the slope of the Changshanhao mine, and its lithology is relatively hard. Also, the energy dissipation layer consisting of gravel with a diameter of 10–30 cm is laid on the platform below the initial motion point of rockfalls, reducing the COR of the platform surface. According to the engineering geological conditions of the Changshanhao mine and the empirical value of COR in some projects (Koleini *et al.* 2011,

Fig. 7 Distribution of rockfalls in Changshanhao open-pit mine

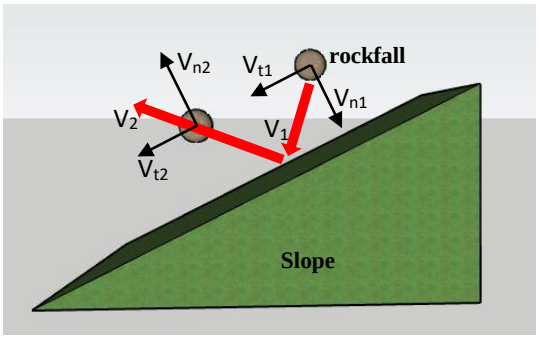

Fig. 8 Motion model of rockfall

Table 2 COR recommended by the Ministry of Railway in China

Slope surface features	Normal COR R_n	Tangential COR R_t
Slope surface is smooth and hard	0.37-0.42	0.87–0.92
Slope surface mostly is bedrock and conglomerate	0.33-0.37	0.83–0.87
Hard soil slope	0.30-0.33	0.80–0.83
Soft soil slope	0.28-0.30	0.78–0.80

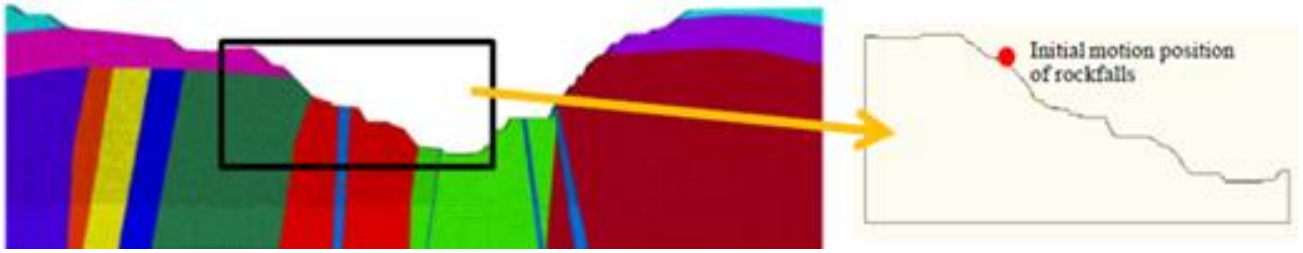

(a)

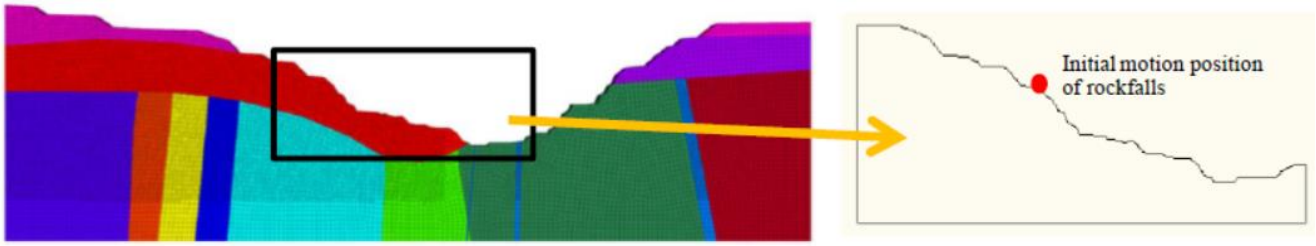

(b)

Fig. 9 Selected area for motion analysis of rockfalls (a) W6 section slope and (b) W8 section slope

Saroglou *et al.* 2012), referring to the normal and tangential COR recommended by the Transport Bureau of the Ministry of Railway in China (Table 2), the basic parameters of this calculation are as follows: The normal COR (*Rn*) of the hard slope surface was 0.42, and the normal standard deviation was 0.04. The tangential COR (*Rt*) was 0.92, and the tangential standard deviation was 0.04. The friction angle was 32 degrees. The normal COR (*Rn*) was 0.35, and

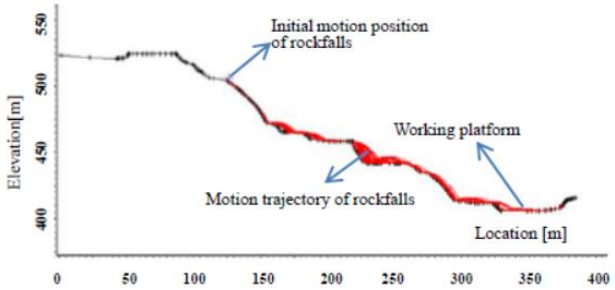

Fig. 9 Motion trajectory of rockfalls on W6 section slope

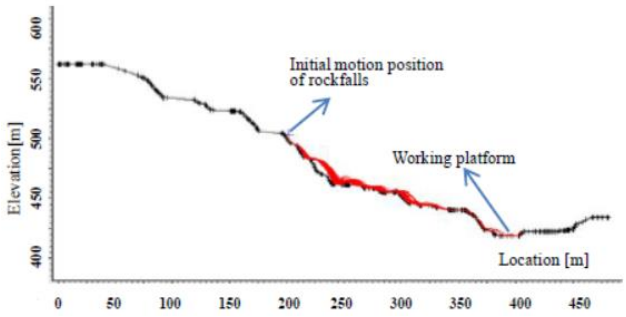

Fig. 10 Motion trajectory of rockfalls on W8 section slope

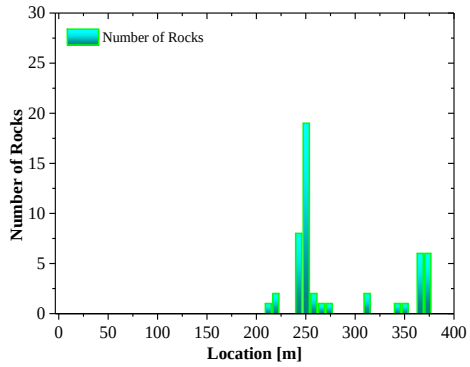

(a)

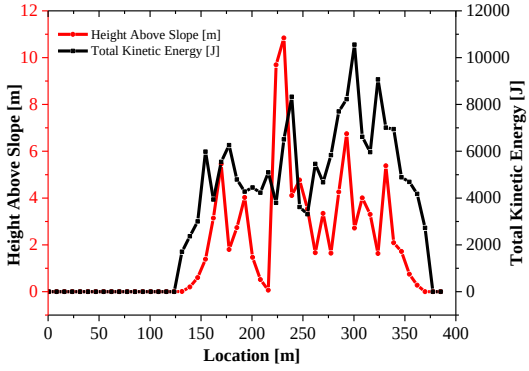

(b)

Fig. 11 Motion characteristics of rockfalls on W6 section slope under normal circumstance: (a) landing distribution and (b) bouncing height and total kinetic energy

the normal standard deviation was 0.04. The tangential COR (*Rt*) was 0.85, and the tangential standard deviation was 0.04. The friction angle was 30 degrees.

The left side of the slopes of the two sections was

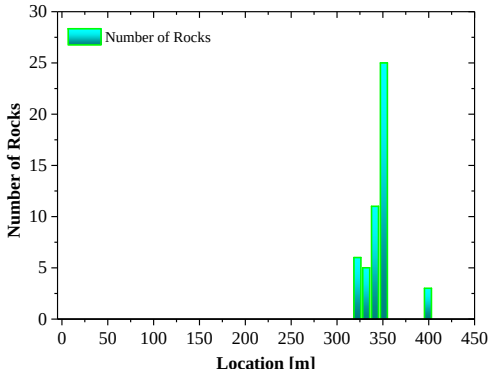

(a)

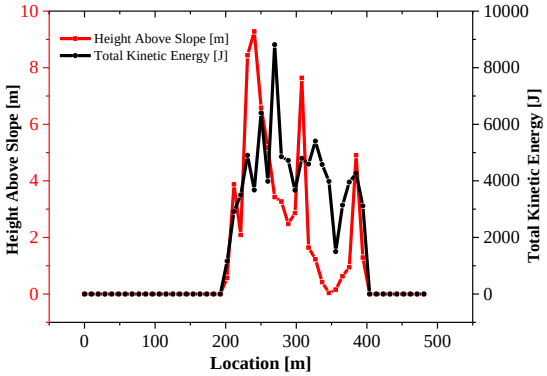

(b)

Fig. 12 Motion characteristics of rockfalls on W8 section slope under normal circumstance: (a) landing distribution and (b) bouncing height and total kinetic energy

selected to analyze the motion characteristics of rockfalls (Fig. 8). The parameters of each section of slope were set according to the actual geological situation of the field. According to the results from the analysis of slope stability, the position of the initial motion of rockfalls was assumed to be at a 125 m horizontal distance from the current slope top (W6 section slope) and at a 209 m horizontal distance from the current slope top (W8 section slope).

According to the field distribution of rockfalls, it was assumed that 50 rockfalls moved from the position of the initial motion. The average mass of the rockfalls was 35 kg, and the standard deviation was 1 kg. The pseudo-random method was used in the numerical simulation of rockfall. The motion trajectories of rockfalls on the slopes of the W6 and W8 sections are shown in Figs. 9 and 10.

As shown in Figs. 9 and 10, a large number of rockfalls accumulated on the working platform at the bottom of the stope, and this severely affected the safety of the mine. Therefore, protective measures are needed to control rockfalls. In the motion of rockfalls, the landing distribution, bouncing height (*H*, the height of a rockfall relative to the slope surface), and total kinetic energy (*J*) of rockfalls are important parameters for determining the location and type of protective measures. Therefore, this study focuses on the evaluation of these parameters. The landing distribution, bouncing height, and total kinetic energy of rockfalls in W6 and W8 section slopes are shown in Figs. 11 and 12, respectively.

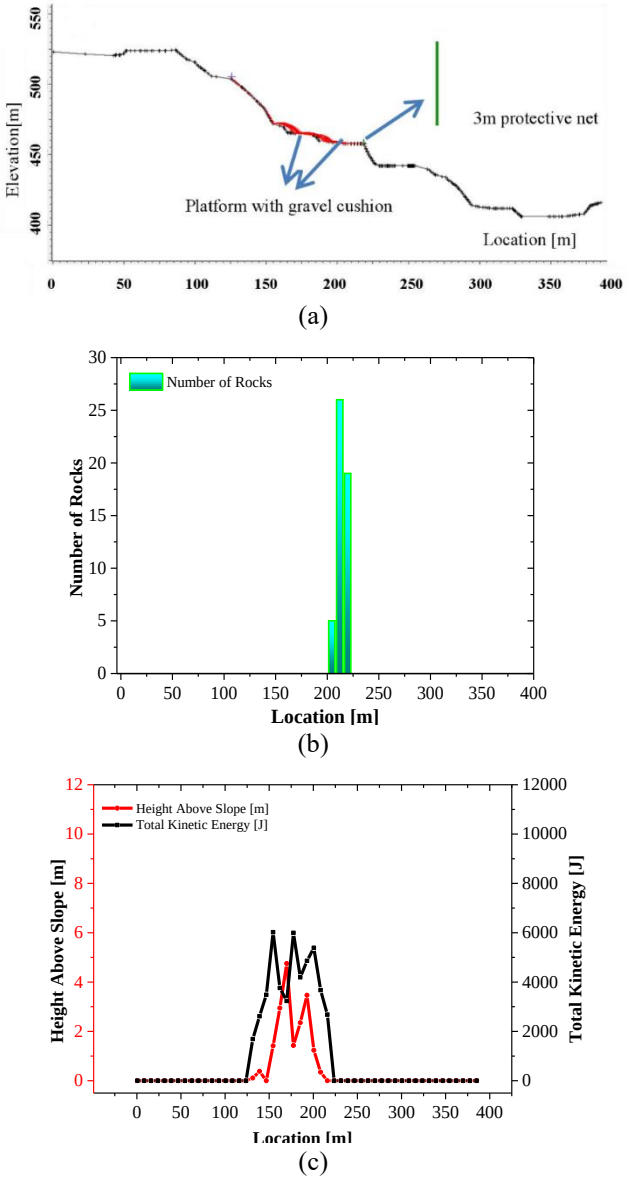

Fig. 13 Motion characteristics of rockfalls on W6 section slope after using protective methods (a) Motion trajectory, (b) Landing distribution and (c) Bouncing height and total kinetic energy distribution

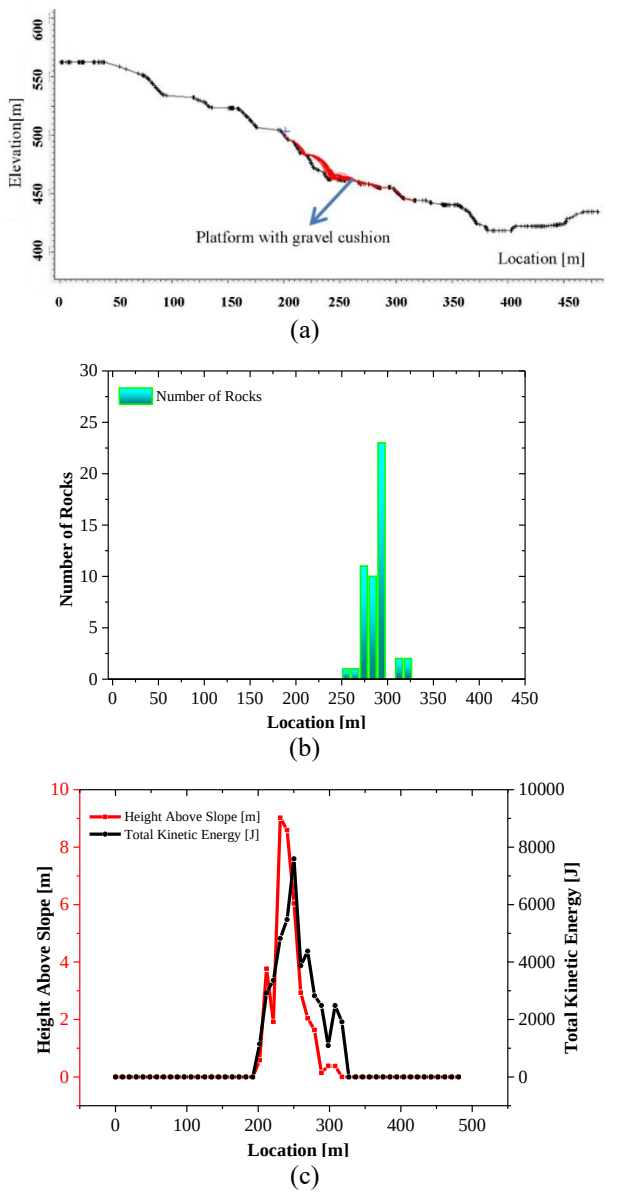

Fig. 14 Motion characteristics of rockfalls on W8 section slope after using protective methods (a) Motion trajectory, (b) Landing distribution and (c) Bouncing height and total kinetic energy distribution

The bouncing height and total kinetic energy are important parameters of the motion characteristics of rockfalls. As seen in Figs. 11(b) and 12(b), the kinetic energy and bouncing height of rockfalls on the slopes of the W6 and W8 sections are relatively large during rolling. The total kinetic energy curve continuously increases when the rockfalls move from the top of the slope. However, the bouncing height is very small, and this indicates that the rockfalls are in the sliding stage at this time. Before the collision between the rockfall and mass of the slope rock, the total kinetic energy curve gradually increases. After collision, the rockfall rebounds and rises. The kinetic energy is transformed into potential energy, and the total kinetic energy curve of the rockfall decreases. Overall, the location of rockfalls on the slope of the W6 section is higher than those on the slope of the W8 section. The potential energy of rockfalls on the slope of the W6 section is relatively high. Thus, the rockfalls have high kinetic energy and a high bouncing height during rolling.

4.3 Effects of control methods

Usually, it is easier to intercept rockfalls by setting a protective net near the initial motion point of rockfall. However, in actual engineering, it is difficult to build high protective nets to control rockfalls that have high kinetic energy because of the high cost and complex construction of protective nets. A lot of waste rocks are produced during mine expansion. This method uses waste rocks, which lay on a platform below the initial moving point of rockfalls, as an energy dissipation layer. This reduces the COR of the platform surface when rockfalls move through the platform.

Fig.15 Interception effect of a platform paved with a gravel cushion for rockfall disasters

Therefore, laying a gravel cushion that consists of gravel with a diameter of 10-30 cm on a platform below the initial motion point can effectively reduce the kinetic energy and bouncing height and improve the safety of a mine. Laying a gravel cushion can also avoid the cost of transporting waste stones, which provides some economic benefit.

Because the platform with a gravel cushion in the W6 section slope is relatively narrow, two platforms below the point of the initial motion were paved with a gravel cushion, and a 3-m protective net was built at the rear edge of the second platform to guarantee the safety of workers and equipment. Although the potential energy of rockfalls in the W8 section slope is relatively low, the platform was paved with a gravel cushion below the point of the initial motion without a retaining wall. After using protective methods, the achieved trajectory of motion, landing distribution, bouncing height, and total kinetic energy of rockfalls are shown in Figs. 13 and 14.

From a comparison of numerical results before and after using protective methods, it was found that the total kinetic energy and bouncing height of rockfalls decrease after a gravel cushion was laid. Also, the landing position of rockfalls is closer to the point of the initial motion. For the W6 section slope, after rockfalls pass through two platforms paved with gravel cushion, the bouncing height of rockfalls at a 208 m distance from the slope top is 0.35 m with a kinetic energy of 3673 J; these can be easily intercepted by a 3-m protective net located at a 220 m distance from the top of the slope. For the W8 section slope, the rockfalls were finally intercepted after they passed through a platform paved with a gravel cushion. The bouncing height (H) and total kinetic energy (J) finally became zero. This proves that the protective methods are effective at controlling rockfall disasters, guaranteeing the safety of workers and equipment on the working platform.

4.4 Results verification

To validate the effectiveness of the proposed prevention method, a typical slope in open-pit mines is selected as a testing area. The upper area in the slope is seriously weathered and prone to collapse, and platforms with a width of 2-4 m were excavated. Under an artificial disturbance, many blocks fell onto the working site. During the mine expansion process, many waste rocks are produced. These waste rocks were broken into small sizes particles and laid on platforms as a protective cushion. Many rockfalls are intercepted on the platform paved with the gravel cushion, and there are basically no rockfalls that roll down to the working site, as shown in Figure 15. The prevention methods make use of waste rocks that are produced in the mine expansion process; this reduces the prevention costs and solves to some extent the problem of dump accumulation. This approach keeps workers and equipment away from the threat of rockfall and greatly improves the work efficiency of the open-pit mining industry.

5. Conclusions

In this study, the slope stability of the Changshanhao open-pit mine was analyzed to identify the high-incidence area of rockfalls. Also, the rationality and reliability of measures used to control rockfalls were verified using Rocfall software. The following conclusions can be drawn:

(1) Through slope stability analysis of each section of the Changshanhao open-pit mine, the vulnerable slope area was determined, especially for the W6 and W8 slopes, and the dangerous rock mass in the vulnerable area was serious. Thus, the vulnerable slope area is considered to be a high-incidence area of rockfalls, and the unstable rock mass in these areas should be reinforced to prevent rockfalls from the source.

(2) Rocfall software was used to simulate the motion trajectory of rockfalls; 16 rockfalls stopped on the working platform in the W6 slope, and 3 blocks stopped on the working platform in the W8 slope. The total kinetic energy (J), bouncing height (H), and landing distribution position of rockfalls during rolling were determined. In the W6 slope, the maximum value of H is 10.8 m, and the maximum value of J is 10544 J. In the W8 slope, the maximum value of H is 9.28 m, and the maximum value of J is 8813 J. This provides a reliable reference for determining different protective measures and their control effects.

(3) According to the different positions of vulnerable slope areas, different treatment measures are proposed. For vulnerable slope areas that are at a higher position, it is advisable to lay a gravel cushion on the lower platform to reduce the kinetic energy and bouncing height of rockfalls and to build a protective net at the rear edge of platform for double protection because of the high potential energy. For vulnerable slope areas that are at a lower position, an excellent control effect can be achieved by only laying a gravel cushion on the lower platform. After setting prevention methods, the maximum value of H was 4.75 m, and the maximum value of J was 6019 J in the W6 slope; the maximum value of H was 9 m, and the maximum value of J was 7596 J in the W8 slope. Also, all of the rockfall was intercepted above the working platform. The rationality and effectiveness of these methods were verified via numerical simulation. This work provides a good basis for scientific prevention and control of rockfalls.

Acknowledgments

This work was supported by the National Natural Science Foundation of China (52104125), the Fundamental Research Funds for the Central Universities (No. B210201001) and the Technology top talent support project of Guizhou Provincial Education Department ([2020]155), Research and development project of Guizhou University of Engineering Science (Grant No: G2018016), Bijie city science and technology plan joint fund project ([2019]26).

Data availability statement

The data are available and are explained in this article. Readers can access the data supporting the conclusions of this study.

References

Andrew, M. and Oldrich, H. (2017), "Theory and calibration of the Pierre 2 stochastic rock fall dynamics simulation program", *Can. Geotech. J.*, **54**(1), 18-30. https://doi.org/10.1139/cgj-2016-0039.

Anna, E., Klaus, T., Anna, G. and Corinna, W. (2017), "Efficient discrete modelling of composite structures for rockfall protection", *Comput. Geotech.*, **87**, 99-114. https://doi.org/10.1016/j.compgeo.2017.02.005.

Akin, M., Dincer, I., Ok, A.O., Orhan, A., Akin, M.K. and Topal, T. (2021), "Assessment of the effectiveness of a rockfall ditch through 3-D probabilistic rockfall simulations and automated image processing", *Eng. Geol.*, **283**, 106001. https://doi.org/10.1016/j.enggeo.2021.106001.

Bourrier, F., Dorren, L., Nicot, F., Berger, F. and Darve, F. (2009), "Toward objective rockfall trajectory simulation using a stochastic impact model", *Geomorphology*, **110**(3), 68-79. https://doi.org/10.1016/j.geomorph.2009.03.017.

Buzzi, O., Giacomini, A. and Spadari, M. (2012), "Laboratory investigation on high values of restitution coefficients", *Rock Mech. Rock Eng.*, **45**, 35-43. https://doi.org/10.1007/s00603-011-0183-0.

Bhatti, A.Q. (2018), "Computational modeling of energy dissipation characteristics of expanded polystyrene (EPS) cushion of reinforce concrete (RC) bridge girder under rockfall impact", *Int. J. Civ. Eng.*, **16**(11), 1-8. https://doi.org/10.1007/s40999-018-0304-1.

Bertolo, P., Oggeri, C. and Peila, D. (2009), "Full-scale testing of draped nets for rock fall protection", *Can. Geotech. J.*, **46**(3), 306-317. https://doi.org/10.1139/T08-126.

Fanos, A.M. and Pradhan, B. (2019), "A novel rockfall hazard assessment using laser scanning data and 3D modelling in GIS", *Catena*, **172**, 435-450. https://doi.org/10.1016/j.catena.2018.09.012.

Gischig, V.S., Hungr, O., Mitchell, A. and Bourrier, F. (2014), "Pierre3D: A 3D stochastic rockfall simulator based on random ground roughness and hyperbolic restitution factors", *Can. Geotech. J.*, **52**(9), 1360-1373. https://doi.org/10.1139/cgj-2014-0312.

Gao, G. and Meguid, M.A. (2018a.), "Modeling the impact of a falling rock cluster on rigid structures", *Int. J. Geomech.*, **18**(2), 1-15. https://doi.org/10.1061/(ASCE)GM.1943-5622.0001045.

Gao, G. Meguid, M.A. (2018b), "On the role of sphericity of falling rock clusters- Insights from experimental and numerical investigations", *Landslides*, **15**(2), 219-232. https://doi.org/10.1007/s10346-017-0874-z

Hu, J., Li, S.C., Shi, S.S., Li, L.P., Zhang, Q., Liu, H.L. and He, P. (2018), "Experimental study on parameters affecting the runout range of rockfall", *Adv. Civ. Eng.*, 1-9. https://doi.org/10.1155/2018/4739092.

James, G. (2015), "Rock-shape and its role in rockfall dynamics", Ph.D. Dissertation, Durham University, Durham., U.K.

Koo, R.C.H., Kwan, J.S.H., Lam, C., Ng, C.W.W., Yiu, J., Choi, C.E., Ng, A.K.L., Ho, K.K.S. and Pun, W.K. (2017), "Dynamic response of flexible rockfall barriers under different loading geometries", *Landslides*, **14**(3), 905-916. https://doi.org/10.1007/s10346-016-0772-9.

Koleini, M., Van, R.J.L. (2011), "Falling rock hazard index: A case study from the Marun Dam and power plant, south-western Iran", *B. Eng. Geol. Environ.*, **70**(2), 279-290. https://doi.org/10.1007/s10064-010-0327-6.

Lam, C., Yong, A.C.Y., Kwan, J.S.H. and Lam, N.T.K. (2018), "Overturning stability of L-shaped rigid barriers subjected to rockfall impacts", *Landslides.*, **15**(7), 1347-1357. https://doi.org/10.1007/s10346-018-0957-5.

Li, L.P., Sun, S.Q., Li, S.C., Zhang, Q.Q., Hu, C. and Shi, S.S. (2016), "Coefficient of restitution and kinetic energy loss of Rockfall impacts", *KSCE J. Civ. Eng.*, **20**(6), 2297-2307. https://doi.org/10.1007/s12205-015-0221-7.

Lambert, S. and Kister, B. (2018), "Efficiency assessment of existing rockfall protection embankments based on an impact strength criterion", *Eng. Geol.*, **243**, 1-9. https://doi.org/10.1016/j.enggeo.2018.06.008.

Laura, C.J., Elena, B.F., Daniel, C.F. and Diego, F. (2018) "Use of explicit FEM models for the structural and parametrical analysis of rockfall protection barriers", *Eng. Struct.*, **166**, 212-216. https://doi.org/10.1016/j.engstruct.2018.03.064.

Maerz, N.H., Youssef, A.M., Pradhan, B. and Bulkhi, A. (2015), "Remediation and mitigation strategies for rock fall hazards along the highways of Fayfa Mountain, Jazan Region, Kingdom of Saudi Arabia", *Arab. J. Geosci.*, **8**(5), 2633-2651. https://doi.org/10.1007/s12517-014-1423-x.

Megan, V.V., Hutchinson, D.J., Bonneau, D.A., Sala, Z., Ondercin, M. and Lato, M. (2018), "Combining temporal 3D remote sensing data with spatial rockfall simulations for improved understanding of hazardous slopes within rail corridors", *Nat. Hazard. Earth. Syst.*, **18**(8), 2295-2308. https://doi.org/10.5194/nhess-18-2295-2018.

Rosa, M.M., Inmaculada, G.M., Paola, R., Gerardo, H., Roberto, S., Joan, R., Raúl, A. and Federica, F. (2016), "Calibration and validation of rockfall modelling at regional scale: application along a roadway in Mallorca (Spain) and organization of its management", *Landslides*, **13**(4), 751-763. https://doi.org/10.1007/s10346-015-0602-5.

Saroglou, H., Marinos, V., Marinos, P. and Tsiambaos, G. (2012), "Rockfall hazard and risk assessment: An example from a high promontory at the historical site of Monemvasia, Greece", *Nat. Hazard. Earth. Syst.*, **12**(6), 1823-1836. https://doi.org/10.5194/nhess-12-1823-2012.

Spadari, M., Giacomini, A., Buzzi, O., Fityus, S. and Giani, G.P. (2012), "In situ rock fall tests in New South Wales, Australia", *Int. J. Rock Mech. Min. Sci.*, **49**, 84-93. https://doi.org/10.1016/j.ijrmms.2011.11.013.

Toe, D., Mentani, A., Govoni, L., Bourrier, F., Gottardi, G. and Lambert, S. (2018), "Introducing Meta-models for a more efficient hazard mitigation strategy with rockfall protection barriers", *Rock Mech. Rock Eng.*, **51**(4), 1097-1109. https://doi.org/10.1007/s00603-017-1394-9.

Tan, D.Y., Yin, J.H., Qin, J.Q., Zhu, Z.H. and Feng, W.Q. (2018), "Large-scale physical modeling study on the interaction between rockfall and flexible barrier", *Landslides*, **15**(12), 2487-2497. https://doi.org/10.1007/s10346-018-1058-1.

Tao, Z.G., Geng, Q., Zhu, C., He, M.C., Cai, H., Pang, S.H. and Meng, X.Z. (2019), "Investigation of the mechanical mechanisms of large-scale toppling failure on counter-inclined rock slopes", *J. Geophys. Eng.*, **16**, 541-558. https://doi.org/10.1093/jge/gxz020.

Tao, Z.G., Zhu, C., He, M.C. and Liu, K.M. (2020), "Research on the safe mining depth of anti-dip bedding slope in Changshanhao Mine", *Geomech. Geophys. Geo.* **6**, 36. https://doi.org/10.1007/s40948-020-00159-9.

Xu, H., Gentilini, C., Yu, Z.X., Qi, X. and Zhao, S.C. (2018), "An energy allocation based design approach for flexible rockfall protection barriers", *Eng. Struct.*, **173**, 831-852. https://doi.org/10.1016/j.engstruct.2018.07.018.

Yilmaz, I., Yildirim, M. and Keskin, I. (2008), "A method for mapping the spatial distribution of RockFall computer program analyses results using ArcGIS software", *B. Eng. Geol. Environ.*, **67**, 547-554. https://doi.org/10.1007/s10064-008-0174-x.

Yu, Z.X., Luo, L.R., Liu, C., Guo, L.P., Qi, X. and Zhao, L. (2021), "Dynamic response of flexible rockfall barriers with different block shapes", *Landslides*, 1-17. https://doi.org10.1007/s10346-021-01658-w

Zhang, G., Tang, H., Xiang, B., Karakus, B. and Wu J.P. (2015), "Theoretical study of rockfall impacts based on logistic curves", *Int. J. Rock Mech. Min. Sci.*, **78**, 133-143. https://doi.org/10.1016/j.ijrmms.2015.06.001.

Zhu, C., Tao, Z., Yang, S. and Zhao, S. (2019), "V shaped gully method for controlling rockfall on high-steep slopes in China", *B. Eng. Geol. Environ.*, **78**, 2731-2747. https://doi.org/10.1007/s10064-018-1269-7.

Zhu, C., Wang D.S., Xia, X., Tao, Z.G., He, M.C. and Cao, C. (2018), "The effects of gravel cushion particle size and thickness on the coefficient of restitution in rockfall impacts", *Nat. Hazard. Earth. Syst.*, **18**(6), 1811-1823. https://doi.org/10.5194/nhess-18-1811-2018.

Zhu, C., He, M.C., Karakus, M., Cui, X.B. and Tao, Z.G. (2020), "Investigating toppling failure mechanism of anti-dip layered slope due to excavation by physical modelling", *Rock Mech. Rock Eng.*, **53**(11), 5029-5050. https://doi.org/10.1007/s00603-020-02207-y.

Zhu, C., He, M.C., Karakus, M., Zhang, X.H. and Guo, Z. (2021a), "The collision experiment between rolling stones of different shapes and protective cushion in open-pit mines", *J. Mt. Sci. Eng.*, **18**(5), 1391-1403. https://doi.org/10.1007/s11629-020-6380-0.

Zhu, C., He, M.C., Yin, Q. and Zhang, X.H. (2021b), "Numerical simulation of rockfalls colliding with a gravel cushion with varying thicknesses and particle sizes", *Geomech. Geophys. Geo.*, **7**(1), 1-15. https://doi.org/10.1007/s40948-020-00203-8.

Zhu, C., He, M.C., Karakus, M., Zhang, X.H. and Tao, Z.G. (2021c), "Numerical simulations of the failure process of anaclinal slope physical model and control mechanism of negative Poisson's ratio cable", *B. Eng. Geol. Environ.*, **80**, 3365-3380. https://doi.org/10.1007/s10064-021-02148-y.

Zhao, P., Xie, L.Z., Li, L.P., Liu, Q. and Yuan, S. (2018), "Large-scale rockfall impact experiments on a RC rock-shed with a newly proposed cushion layer composed of sand and EPE", *Eng. Struct.*, **175**, 386-398. https://doi.org/10.1016/j.engstruct.2018.08.046.